

# Advances in X-ray Microfocusing with Monocapillary Optics at CHESS

Sterling W. Cornaby<sup>1,2,3</sup>, Thomas Szebenyi<sup>1</sup>, Heung-Soo Lee<sup>4</sup>, and Donald H Bilderback<sup>1,2</sup>

<sup>1</sup>Cornell High Energy Synchrotron Source, Cornell University

<sup>2</sup>Applied and Engineering Physics, Cornell University

<sup>3</sup>Currently at Moxtek Inc., Orem, UT

<sup>4</sup>Pohang Accelerator Laboratory, Pohang, Korea

Single-bounce monocapillary optics are elliptically-shaped hollow glass tubes which are capable of focusing x-ray beams at CHESS to a spot size between 5 and 50  $\mu\text{m}$ , with intensity gains ranging from 10 to 1000, and divergences ranging from 1 to 10 milliradians (mr)<sup>1,2,3</sup>. Experiments at CHESS using x-ray microbeams created with these optics include high pressure powder diffraction, high resolution micro-diffraction ( $\mu\text{XRD}$ )<sup>4,5</sup>, micro-x-ray fluorescence ( $\mu\text{XRF}$ )<sup>6,7</sup>, micro-XANES<sup>8</sup>, confocal x-ray fluorescence on antique paintings (confocal  $\mu\text{XRF}$ )<sup>9</sup>, micro-protein crystallography<sup>10</sup>, Laue protein crystallography<sup>11</sup>, micro-small angle x-ray scattering ( $\mu\text{SAXS}$ )<sup>12</sup>, time-resolved powder diffraction of reactive multilayer foils<sup>13</sup>, miniature toroidal mirrors for grazing-incidence SAXS<sup>14</sup>, micro-X-ray standing waves<sup>18</sup>, and others<sup>15</sup>.

Over the past few years, experiments using microbeams on various stations at CHESS have increased greatly. Between 2005 and the present, CHESS has increased its hardware to accommodate from one to five simultaneous capillary setups, with specialty setups for protein crystallography and  $\mu\text{SAXS}$ . The increase in x-ray microbeam capacity has been fueled by user requests. During a typical run, one or two x-ray microbeam setups are in use continually throughout the run, with a peak of four of CHESS's twelve stations using x-ray microbeams simultaneously in November 2007.

Single-bounce monocapillaries are shaped like a small section of a very eccentric ellipsoid. Rays emitted from an x-ray source at one focus of an ellipse are directed to the opposite focus where the sample under study is placed, as the rays undergo a single specular reflection from the inner capillary wall. The ellipsoidal shape is designed to satisfy the grazing incidence requirement needed for total external reflection of x-rays. This basic premise allows for many potential shapes for optics that depend on the maximum divergence chosen, spot size required and working length from capillary tip to focus. For synchrotron applications, the source is typically located many meters away from the optic and the incident radiation has a low glancing angle on the glass wall of order  $0.2^\circ$ .

We evaluate the quality of our drawn optics with 4 kinds of tests. First, we evaluate the departure of the observed glass figure from the ideal design shape. This is accomplished using optical metrology to evaluate the rms slope errors and rms centerline deviations from a straight line. Second, we observe a far-field image on a fluorescent screen to measure the divergence of the capillary and to see if it has the proper ring structure. The far-field x-ray image is viewed on a high quality fluorescent screen about 25 to 100 cm downstream from the focus. This far-field image is used to align the optic with the x-ray beam and contains information regarding the straightness and the slope errors of the optic. Third, we take a pinhole scan at the focus of the optic to see that it makes a small spot. The spot size is measured by scanning a 5 to 10  $\mu\text{m}$  diameter pinhole across the focus. Fourth and last, we measure the x-ray beam intensity through the small pinhole with an ion chamber, with and without a capillary. The gain is simply the ratio of the two intensity numbers.

Figure 1 shows both a pinhole scan and a far-field image from a single-bounce monocapillary optic.

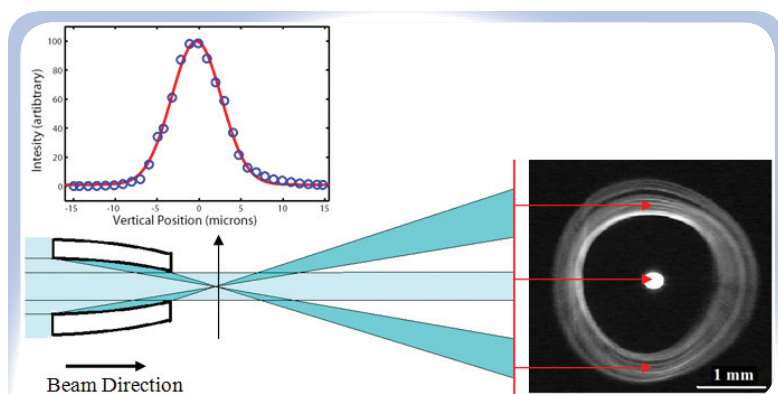


**Fig 1:** A schematic cut away of a single-bounce monocapillary is in the lower left corner. The positions of the reflected rays are in dark blue and positions of the non-reflected rays are in light blue. In the upper left corner is a pinhole scan across the focus of an optic, with a spot size of 5  $\mu\text{m}$  FWHM, determined after deconvoluting the data with the 5  $\mu\text{m}$  pinhole size. A far-field image is on the right side. In the schematic, the far-field screen is represented by the red line, which is normal to the x-ray beam. Both the scan and the far-field image are from capillary f1b\_mr9f20\_01. Note that the outer ring is not perfectly round. The strands of concentric intensity arise from several periods of slight oscillations that develop around the desired figure, most likely imprinted during the drawing process itself. The diagram was taken from reference [1].

Single-bounce monocabillaries have a number of attributes, listed below.

The positive attributes:

- They are achromatic. They reflect all x-ray energies to the same focal spot position.
- They are optically and mechanically robust. For example, they are not particularly fragile and they are typically operated in air.
- They are 90% to 99% efficient. Almost all the x-rays that hit the surface of the optic are reflected, if the condition of total external reflection is satisfied.
- The divergence and focal length can be designed.

The limiting monocabillary attributes are:

- They have profile and slope errors, which currently limit the spot size to 5  $\mu\text{m}$  or larger, at CHESS, with the present glass drawing technology.
- They are not imaging optics, they simply focus the beam.
- They have finite aperture size of about 1 mm or less and divergence of about 12 mrad or less. The small numerical aperture limits the amount of x-ray light that the optic can collect.

Being achromatic, however, is an exceptionally important advantage of the monocabillary optics. This means the focal spot size, the focal spot location, and the divergence of the focused beam do not change with the x-ray photon energy. Thus these optics focus a 0.01% bandwidth beam as effectively as a 50% bandwidth beam. The reflection efficiency remains high over the entire x-ray energy range as long as the x-rays do not exceed the critical angle.

A recent example of using this achromatic principle to good advantage can be seen in a Laue diffraction experiment whose purpose is to determine the 3D crystal structure of protein microcrystals<sup>1,16</sup>. This experiment used a combination of two rhodium coated reflection mirrors and a silicon nitride x-ray transmission mirror to generate a 30% bandwidth beam peaked at 12 keV, Figures 2 and 3.

The wide-bandwidth beam was then focused with a single-bounce monocabillary optic to a 10(H)x13(V)  $\mu\text{m}^2$  spot, with a divergence of  $\sim 5(\text{H})\times 2(\text{V})$  mrad<sup>2</sup> and resulted in a total flux of  $4.4\times 10^{10}$  photons/s ( $\sim 3.4\times 10^8$  photons/s/ $\mu\text{m}^2$  over the 30% bandwidth). This experiment was performed at the D1 bending magnet station whose critical energy is about 10 keV.

The flux density achieved using the bending magnet is close to what you would expect for a 1-2% bandwidth microfocused beam on a wiggler station. This small beam was then used to take Laue diffraction images of small protein crystals, mostly lysozyme, but also of a few thaumatin crystals, Figure 4.

The crystals were a few tens of microns in size. In the short term, we believe that this approach will lead to a new avenue for solving protein structures using less than 10  $\mu\text{m}$  sized crystals at CHESS. In the longer term at an ERL source of x-rays, we hope to push crystal sizes down into the hundreds of nanometers range with this approach - an approach that will be more limited by the radiation damage of crystals than by any beam qualities.

Another important advantage of single-bounce monocabillary optics is that the divergence and focal length can be designed. CHESS has a glass capillary puller which has been set up to make a number of different optics<sup>1</sup>. Two examples show the power of having this in-house tool for constructing specialized monocabillary optics. We have been able to fabricate "football" shaped optics with very short focus-to-focus distances of 20 to 30 cm<sup>1</sup>. We have also been able to make a bifocal miniature toroidal mirror that horizontally and vertically focuses to two different locations<sup>14</sup>.

The need for a football monocabillary optic arose within the Confocal X-Ray Fluorescence (CXRF) project, led by CHESS staff scientist Arthur Woll and his collaborators, to investigate buried paint layer structures of antique paintings<sup>9</sup>. CXRF uses x-ray

**Fig. 2:** A diagram of the setup for two total-reflection mirrors and a single 300 nm thick transmission mirror used to create a tunable, large-bandwidth beam for crystallography. The diagram was redrawn from reference [1].

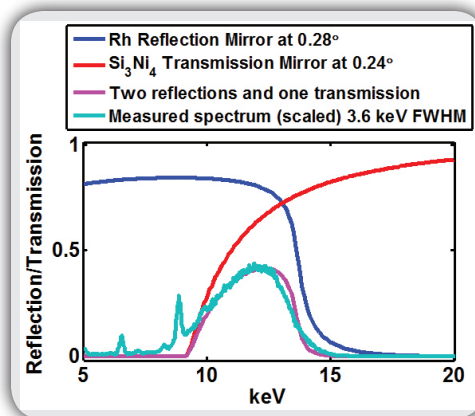
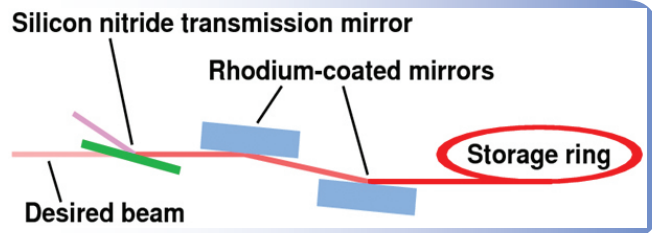


**Fig. 3:** A graph showing the predicted efficiency and measured spectrum of the 30% bandwidth (FWHM) created from two rhodium reflection mirrors and one  $\text{Si}_3\text{N}_4$  transmission mirror combination. The pink curve is calculated, and the blue-green curve is measured. They compare favorably. The bandwidth is peaked at 12 keV ( $\lambda=1.24$  Å) with half-height values at 9.6 keV ( $\lambda=1.29$  Å) and 13.4 keV ( $\lambda=0.93$  Å). In the measured Compton scattering curve (green), the several sharp fluorescence peaks originate from trace contaminants within the Kapton<sup>®</sup> tape; they are not present in the incident X-ray beam. The diagram was taken from reference [1].

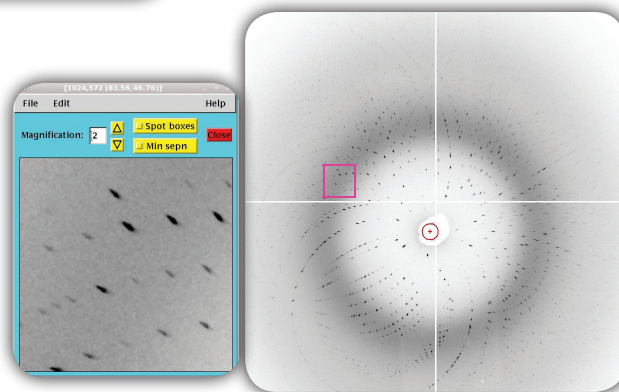


**Fig. 4:** Right, Laue diffraction pattern from a lysozyme crystal. Left, magnified view of the area in the magenta box, showing well-separated, acceptably-shaped spots.

optics to define a small viewable volume in free space that the XRF detector can see. By limiting the volume of the detection region with two separate x-ray optics, the third dimension (the depth) of the sample's elemental composition can be resolved, such as in a painting's underlying layers. At CHESS, a single-bounce monocalipillary optic is used to focus the x-ray beam and an XOS polycapillary optic is used to collect XRF events for the detector, Figure 5.

We decided to try CXRF with two crossed monocalipillary optics. The second collection optic needed to have a very short focus-to-focus distance of 30 cm or less. We made this second football-shaped optic and were able to use it in a CXRF experimental setup to test the confocal resolution, Figure 6.

The football-shaped optic is a good fit for x-ray tube sources, where short focus-to-focus distances improve the total usable x-ray flux from the tube. We are presently looking further into other applications using this kind of optic.

We have also made a non-elliptically shaped single-bounce monocalipillary optic at CHESS. A special dual-focal length toroidal mirror was designed to focus vertically at the sample's position 50 mm from the capillary tip and to horizontally focus at the detector's position, 150 mm from the capillary tip. This mirror was made to provide a smaller vertical footprint of beam for grazing incidence wide-angle scattering (GIWAXS), while at the same time producing better angular resolution in the horizontal direction. No other capillary has been designed to date with such separate focal distances!

This optic, however, is very similar in concept to the elliptically-shaped single-bounce monocalipillary optics. This miniature toroidal mirror was designed to decouple the sagittal and meridional focusing of the traditional single-bounce monocalipillary optic, Figure 7.

Essentially, the normal ellipsoidal shape is modified by increasing its inner diameter, changing the sagittal focus, and at the same time not modifying its meridional curvature, leaving the meridional focusing capability unchanged.

Using the entire inner optical surface will not produce the needed horizontal line focus at the sample position and a vertical line focus at the detector position. In order to create a line focus, only a small section of the optic's full inner surface is exposed to x-rays. Slits are set upstream of the optic to block most of the optical surface illumination as only about 10% of the inner optical surface area is used. [If the full surface of the optic is exposed to an x-ray beam, a narrow ring of intensity will be observed at the location of the meridional focus, and a semi-large spot will appear at the sagittal focused position.] X-ray tests were made with this optic, Figure 8.

Improvements have been made to the capillary drawing process. Parts are now drawn under constant pressure (rather than constant tension) and the furnace moves in the opposite direction to the upward drawing of glass out of the heating zone, Figure 9.

These changes, instituted by Heung-Soo Lee when he was a visiting scientist with

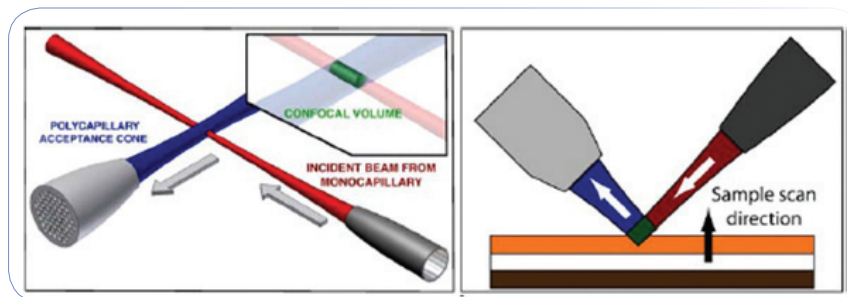


**Fig. 5:** The left diagram shows how a small detection volume in space is created at the intersection of a beam produced by the monocalipillary and accepted by the polycapillary optic. The confocal volume is green in color in the inset. The diagram on the right shows how this small volume can be used to resolve a layered structure. Since the confocal volume is about the same dimension as a typical paint layer on an oil painting, the composition of the different layers can be resolved in three dimensions. The diagram was taken from reference [9].

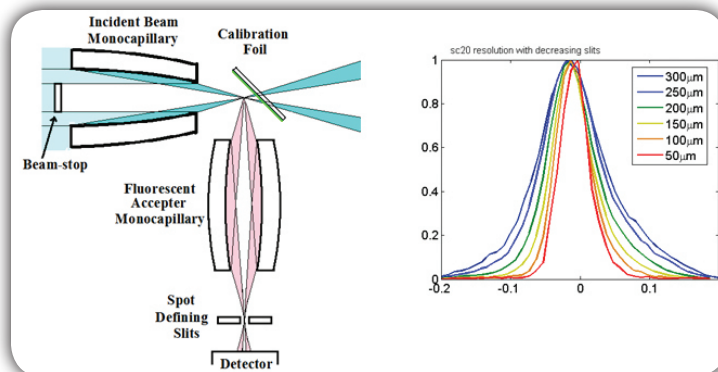


**Fig. 6:** The left diagram shows a sketch of the CXRF test made with two monocalipillary optics. The confocal volume was measured with an XRF detector, as a 6  $\mu\text{m}$  thin lead foil was passed through the confocal volume. Spot defining slits at the second focus of the football shaped collection optic controlled the viewable size of the confocal volume. The graph on the

right shows the resolution as a function of the slit opening. A resolution of  $\sim 120 \mu\text{m}$  FWHM was achieved with a 300  $\mu\text{m}$  slit setting, and a resolution of  $\sim 50 \mu\text{m}$  FWHM was achieved with a 50  $\mu\text{m}$  slit setting. The diagram was taken from reference [1].

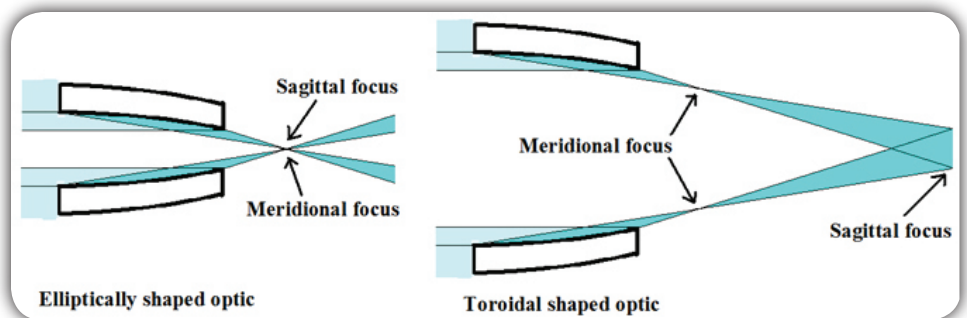


**Fig. 7:** This sketch outlines the morphing of an ellipsoidal shape (left) into a toroidal shape (right). The diameter of the optic is changed, thereby decoupling, the sagittal and meridional focal points. The meridional focus position is unchanged, but the sagittal focusing is moved further away from the tip of the optic. The diagram was taken from reference [14].

us last year, have contributed to drawing better optics. In addition, H-S. Lee also worked on making far-field simulations from the slope errors measured from the on-board Keyence optical metrology, Figure 10.

In conclusion, micro-focusing single-bounce monocapillary optics will continue to be an integral part of the capabilities of CHES. Work will continue to perfect the monocapillary optics by reducing slope and figure errors in the fabrication process. With improvements in slope and figure errors, these optics should make smaller beam sizes and will be very useful for both 3rd generation x-ray sources and the ERL.

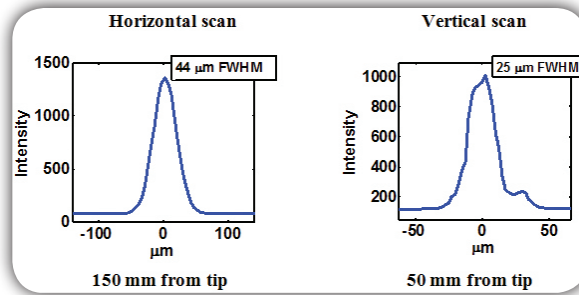


**Fig. 8:** The beam was observed (with 5 micron diameter pinhole scans) to be horizontally focused 150 mm from the capillary tip and vertically focused only 50 mm from the tip, proof that the dual-focal lengths had been produced. Some structure can be seen in the vertical scan, showing that more perfecting work is needed to turn this prototype into a usable optic. Nonetheless, this is an excellent demonstration that a new type of capillary optic has been created! The diagram was taken from reference [14].

**Fig. 9:** Capillary drawing tower showing AB Tech air-bearing in the background, tension-producing stage on the left, furnace and optical metrology in the foreground (with suspended glass tube) and a load cell at the bottom of the apparatus.

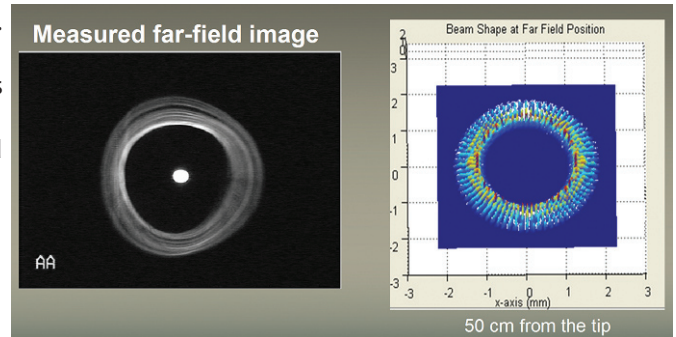
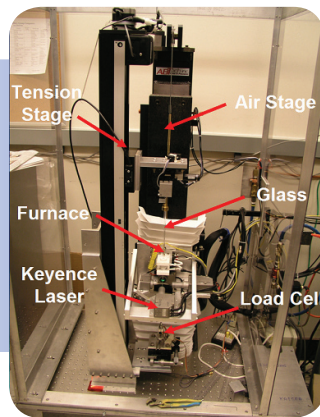


**Fig. 10:** Far-field capillary image (including direct beam in center). Circular strands of intensity are due to small slope errors remaining from the glass drawing process. The simulation on the right shows similar ring structure and is approaching the circular structures seen at left when realistic slope-error values are included in the calculation.

#### Acknowledgement:

We wish to acknowledge that our work was supported by CHES through the NSF & NIH/NIGMS via NSF award DMR-0225180 and by the MacCHES resource through NIH/NCRR award RR-01646. One of us, SC, was also supported by a Cornell University supported G-line fellowship.

#### References:

1. S. Cornaby; The Handbook of X-ray Single-Bounce Monocapillary Optics, Including Optical Design and Synchrotron Applications, Dissertation, Cornell University 2008. Available at [http://glasscal.chess.cornell.edu/Cornaby\\_Capillary\\_Handbook\\_2008.pdf](http://glasscal.chess.cornell.edu/Cornaby_Capillary_Handbook_2008.pdf).
2. S. Cornaby, T. Szebenyi, R. Huang, and D.H. Bilderback; "Design of Single-Bounce Monocapillary X-Ray Optics", 55th Denver X-ray Conference, Advances in X-ray Analysis Vol. 50 (2006)
3. R. Huang and D. H. Bilderback; "Single-bounce Monocapillaries for Focusing Synchrotron Radiation: modeling, measurements and theoretical limits", J. of Synchrotron Radiation 13, 74-84 (2006)
4. A.A. Sirenko, A. Kazimirov, S. Cornaby, D.H. Bilderback, B. Neubert, P. Brueckner, F. Scholz, V. Shneidman, and A. Ougazzaden; "Microbeam High Angular Resolution X-ray Diffraction in InGaN/GaN Selective-area-grown Ridge Structures", Applied Physics Letters 89 (18): Art. No. 181926 (Oct. 30 2006)
5. A. Kazimirov, A.A. Sirenko, D.H. Bilderback, Z.-H. Cai, and B. Lai; "Microbeam High Angular Resolution Diffraction Applied to Optoelectronic Devices", AIP Conference Proceeding CP879, Synchrotron Radiation Instrumentation: Ninth International Conference 1395-1397 (2007)
6. K. Limburg, R. Huang, and D.H. Bilderback; "Fish Otolith Trace Element Maps: new approaches with synchrotron microbeam X-ray fluorescence", X-ray Spectrometry, 36, 336-342 (2007)
7. C. Schmidt, K. Rickers, D.H. Bilderback, and R. Huang; "In situ Synchrotron-radiation XRF Study of REE Phosphate Dissolution in Aqueous Fluids to 800°C", Lithos 95, 87-102 (2007)
8. R.A. Barrea, R. Huang, S. Cornaby, D.H. Bilderback, and T.C. Irving; "High-flux Hard X-ray Microbeam using a Single-bounce Capillary with Doubly Focused Undulator Beam", J. of Synchrotron Radiation 16, 76-82 (2009)
9. A.R. Woll, J. Mass, C. Bisulca, R. Huang, D.H. Bilderback, S. Gruner, and N. Gao; "Development of Confocal X-ray Fluorescence (XRF) Microscopy at the Cornell High Energy Synchrotron Source", Applied Physics A 83 (2), 235-238 (2006)
10. R. Huang and D.H. Bilderback; "Secondary Focusing for Micro-Diffraction using One-Bounce Capillaries", Eighth International Conference on Synchrotron Radiation Instrumentation, AIP Conference Proceedings, 712-715 (2004)
11. Ibid ref. 1
12. J.S. Lamb, S. Cornaby, K. Andresen, L. Kwok, H.Y. Park, X. Qiu, D.M. Smilgies, D.H. Bilderback, and L. Pollack; "Focusing Capillary Optics for use in SAXS", Journal of Applied Crystallography 40, 193-195 (2007)
13. J.C. Trenkle, L.J. Koerner, M.W. Tate, S.M. Gruner, T.P. Weihs, and T.C. Hufnagel; "Phase Transformations during Rapidly Propagating Reactions in Nanolaminated Foils", App. Phys. Lett. vol. 92 (2008)
14. S. Cornaby, D. Smilgies, and D. Bilderback; "Bifocal Miniature Toroidal Shaped X-ray Mirrors", 57th Denver X-ray Conference, Advances in X-ray Analysis Vol. 52 (in print, 2009)
15. D.H. Bilderback, A. Kazimirov, R. Gillilan, S. Cornaby, A. Woll, C-S Zha, and R. Huang; "Optimizing Monocapillary Optics for Synchrotron X-ray Diffraction, Fluorescence Imaging, and Spectroscopy Applications", AIP Conference Proceeding CP879, Synchrotron Radiation Instrumentation: Ninth International Conference, 758-763 (2007)
16. S. Cornaby, D.M.E. Szebenyi, D.M. Smilgies, D.J. Schuller, R. Gillilan, Q. Hao, and D.H. Bilderback, Acta Cryst. D. (submitted)
17. S. Cornaby and D.H. Bilderback; "Silicon Nitride Transmission X-ray Mirrors", Journal of Synchrotron Radiation 15, 371-373 (2008)
18. A. Kazimirov, D.H. Bilderback, R. Huang, A. Sirenko, and A. Ougazzaden; "Microbeam High-resolution Diffraction and X-ray Standing Wave Methods Applied to Semiconductor Structures", J. Phys. D: Appl. Phys. 37, 3L9-L12 (2004)